SF2A 2012
S. Boissier, P. de Laverny, N. Nardetto, R. Samadi, D. Valls-Gabaud and H. Wozniak (eds)

INTEGRAL FIELD SPECTROSCOPY AND GALAXY EVOLUTION

B. Epinat [1]

Abstract. Integral field instruments have an increasing impact on our understanding of galaxy evolution mechanisms. However, these instruments are manifold and each configuration has specific capabilities adapted for different projects. This paper presents various integral field spectroscopy techniques and the main galaxy samples obtained so far, both at low and high redshift. I focus on galaxy kinematics and metallicity studies at high redshift and present their interpretations to understand the evolution of the main mass assembly processes that are merging and continuous cold gas accretion.

Keywords: 3D spectroscopy, galaxy evolution, kinematics, metallicity, high redshift, local universe

1 Introduction

Identifying the processes responsible for galaxy evolution across the cosmic time is crucial to understand the build-up of the Hubble sequence observed in the local Universe. Galaxies at $z \sim 2$ are more star forming than at $z = 0$ (e.g. Tresse et al. 2007) and they are also smaller for a given stellar mass (e.g. Dutton et al. 2011). The main processes invoked nowadays to explain galaxy evolution are mergers on the one hand (e.g. López-Sanjuan et al. 2009), and continuous cold gas accretion on the other hand (e.g. Dekel et al. 2009). In order to study the contribution of these processes along the cosmic time, integral field spectroscopy has become a widely used tool to investigate spatially resolved properties of galaxy samples both locally and at high redshift.

I present a non-exhaustive review on the achievements enabled by integral field spectroscopy on galaxy physics study. Observational constraints are put in regard to the scientific goals and emphasis on the challenges to analyse these data is given. In section 2, the uniqueness of integral field spectroscopy data is explained. Various instrumental concepts and setups that enable to study galaxy physics are also exposed. In section 3, I briefly present the main low and high redshift samples observed using integral field spectroscopy. In section 4, I focus on high redshift galaxy studies and present results obtained so far from kinematics and metallicity analysis that give some insights about galaxy evolution from $z = 3$ to $z = 1$.

2 Integral field spectroscopy techniques

Integral field spectroscopy (IFS) enables to obtain a spectrum for each spatial element of a scientific scene. Concerning galaxy physics analysis, IFS enables to avoid any assumption on the projection parameters: all directions are studied with no preference. For the kinematics, this enables to study non circular motions (e.g. Krajnović et al. 2006). It also allows to detect off axis regions in local galaxy but also companions (e.g. Epinat et al. 2012). At higher redshift, IFS will enable to detect objects with no a priori selection (e.g. MUSE).

The data processing to reconstruct the 3 dimensional information depends on the instrumental concepts. The two main kinds of concepts (in visible and near infra-red wavelengths) are the following:

- Spectral scanning instruments: this is the case of Fabry-Perot instruments (inclusing tunable filters) and Fourier transform spectrographs. Only the spectral information has to be reconstructed. The acquisition is sensitive to sky transparency variations since there is one exposure per spectral element/interferogram.

[1] Laboratoire d'Astrophysique de Marseille, Université d'Aix-Marseille & CNRS, UMR7326, 38 rue F. Joliot-Curie, F-13388 Marseille Cedex 13, France

- Image splitters: this kind of instruments uses optical slicers or microlens arrays to split the field. The field is rearranged using optics or optical fibres and the spectrum is obtain with a grating or a prism that disperse the light. The spatial information has to be reconstructed for these instruments. There can be contaminations from spectrum on a completely different position in the field. Slicers are more subject to these effects than microlens arrays, in particular at the edges of the slices. In addition, slicers are sensitive to the slit effect: the position of the object in the slit modifies slightly the position of the spectrum.

For a constant number of pixels, one has to choose a compromise between the field of view (linked to the spatial sampling) and the spectral range (linked to the spectral sampling). By construction, scanning instruments naturally have large field of view and the number of spectral elements is low whereas spatial splitters have naturally a large number of spectral elements (usually one dimension of the detector) and a smaller field of view. Such configurations have different applications for the study of galaxy physics.

3 Galaxy samples with integral field spectroscopy data

3.1 Samples in the local Universe

In the local Universe, galaxies extend over several arcminutes. IFS thus enables to study the spectral properties with a good spatial resolution (better than 1 kpc up to $z = 0.1$).

SAURON (de Zeeuw et al. 2002) and ATLAS3D (Cappellari et al. 2011) are the main samples that study early type galaxies. ATLAS3D contains 260 galaxies observed with the SAURON instrument, a spatial splitter using microlenses (Bacon et al. 2001). The field of view is around 30" with a spectral resolution around 2000 and a spectral range of $\sim$ 2000Å. These samples are mainly focused on the study of stellar populations and dynamics but the ionised gas is also studied when present in early type galaxies. For these specific data, stellar population models have been developed. These models are fit to the spectrum at each spatial element. One of the main results is the discovery of two dynamical kinds of early type galaxies, fast rotators and slow rotators (Emsellem et al. 2011).

Large samples of late-type galaxies have been built using Fabry-Perot instruments. The main ones are SINGS (Dicaire et al. 2008) and GHASP (Epinat et al. 2008). These observations are focused on gaz dynamics through the study of the Hα line, thus the spectral range is narrow (around 10 Å) but the spectral resolution is large (around 10000) and the field of view is large ($\sim$ 5'$-$10').

3.2 Samples at high redshift

From $z = 0.5$ to $z = 5$, the physical scale only varies between 6 kpc/arcsec and 8.5 kpc/arcsec. Consequently, the spatial resolution is rather low compared to local universe galaxies but galaxies fit in a much smaller field of view of several arcseconds (Fig.1). Adaptive optics enable to reach a much better resolution. However, it requires long integration times, even on 10-m class, telescope due to smaller pixels which reduces severely the sensitivity for extended regions. In addition, high redshift observations are limited to the brightest objects due to the surface brightness dimming that affects extended objects. This induces a decrease of the surface brightness proportional to $(1+z)^4$. Current IFS are not able to observe large sample of galaxies to study stellar populations at high redshift.

On the other side, it is possible to study emission lines, like [OII] in the visible or Hα and [OIII] redshifted in the near infra-red. The main samples are IMAGES ($0.4 < z < 0.8$, Yang et al. 2008), observed using GIRAFFE/VLT (multi integral field units instrument in the optical using microlenses and optical fibers), MASSIV ($0.9 < z < 1.8$, Contini et al. 2012), SINS ($1.3 < z < 2.7$, Förster Schreiber et al. 2009) and LSD/AMAZE ($2.5 < z < 4$, Gnerucci et al. 2010), the three latter observed using SINFONI/VLT (an infrared IFS using an image slicer). A sample has also been built using OSIRIS on the Keck with adaptive optics ($1.5 < z < 2.5$, Law et al. 2009; Wright et al. 2009). The typical spectral resolution of infra-red observations (SINFONI and OSIRIS) is around 2000 while the field of view is limited to around 10" with a typical resolution of 0.6" (seeing-limited observations).

These samples study the Universe across the peak of cosmic star formation activity, period when happens the morphological transition between a variety of complex systems and the well ordered Hubble sequence. However, comparing these samples is not straightforward because they result from various selection functions. Therefore, they are not exactly representative of the underlying populations in each redshift range in the same way. In particular, median SFR decreases from 72M$\odot$, 31M$\odot$ to 7M$\odot$ for SINS, MASSIV and IMAGES.

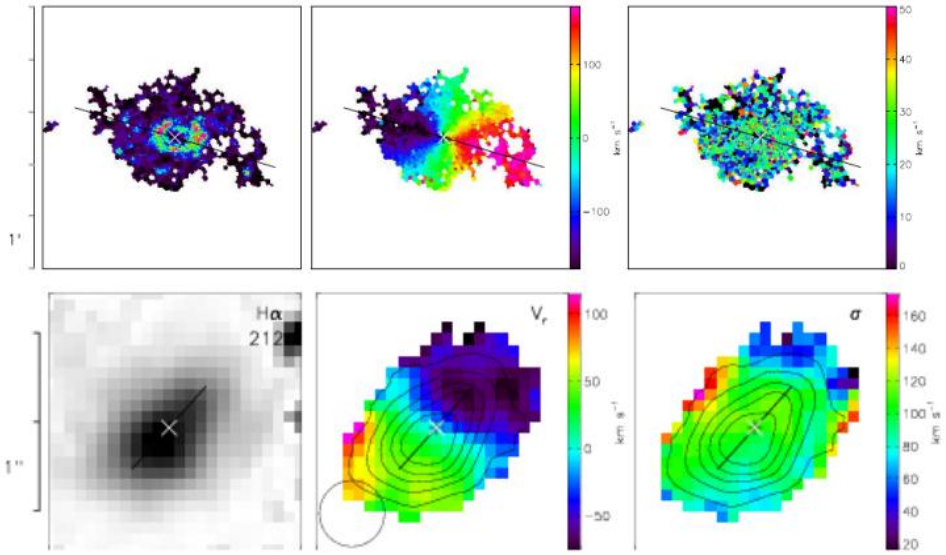

Fig. 1. Example of the comparison between local and high redshift kinematics maps deduced from IFS. Top line: UGC07901 (GHASP sample at $z \sim 0$). Bottom line: VVDS220014252 (MASSIV sample at $z \sim 1.31$). From left to right: Hα line flux map, velocity field and velocity dispersion map. The scale is indicated on the left.

4 Spatially resolved physical properties of high redshift galaxies and galaxy evolution

4.1 Kinematics

High redshift galaxy kinematics are often studied through emission line moment maps (flux, position and width) due to insufficient sensitivity to study stellar kinematics using continuum. Since the typical size of the objects is of the same order than that of spatial PSF, it is necessary to use models that take the spatial resolution into account to recover the true kinematic parameters, such as the rotation velocity and the velocity dispersion. If beam smearing is not considered, the maximum rotation velocity is underestimated and the velocity dispersion is overestimated (peak in the centre due to beam smearing). Epinat et al. (2010) has shown that such models statistically enable to recover these parameters for rotating disk galaxies: they have tested the method on 150 well studied galaxies of the local GHASP sample projected at a similar spatial resolution than SINFONI data of $z \sim 1.5$ galaxies. This method uses a disk thin rotating model convolved by the PSF. Deconvolution methods are still not fully implemented for this specific purpose but are in preparation Dahlia framework[i] for MUSE/VLT.

Kinematics have been used to make classifications of the various samples presented in section 3.2 (Yang et al. 2008; Epinat et al. 2012; Förster Schreiber et al. 2009; Gnerucci et al. 2010). Classes are slightly different among the studies but they roughly distinguish between rotators and galaxies with peculiar kinematics. In some cases, the close environment is probed, giving external indication on interactions. One result is that a large percentage of galaxies among these samples displays peculiar motions away from pure rotation. Signs of interactions are also observed in around 1/3 of each samples. The main sign of evolution is probably the observed decrease of the gaseous velocity dispersion between $\sim$ 80 km/s and $\sim$ 20 km/s from high to low redshift. This may be linked to cold gas accretion mechanism (e.g. Bournaud & Elmegreen 2009) being more efficient at high redshift. An other explanation is that this velocity dispersion is somehow linked to the star-formation regime of the samples (Lehnert et al. 2009; Le Tiran et al. 2011). This has been further supported by IFS observations of galaxies with very high star formation rates ($\sim 20 M\odot$) in the nearby Universe (Green et al. 2010; Gonçalves et al. 2010). Indeed, these local analogues also have large velocity dispersion on average. However, one issue of these studies is the lower spectral resolution ($R < 3000$) of all these observations with respect to reference studies such as GHASP ($R \sim 10000$). The impact of spectral resolution associated to low signal to noise ratio and spatial resolution on the determination of the velocity dispersion has not been studied in detail yet.

[i] https://dahlia.oca.eu/foswiki

4.2 Metallicity

It is possible to estimate metallicity from IFS data using line ratios such as $[NII]/H\alpha$ (e.g. Queyrel et al. 2012) or $[OIII]/[OII]$, $[OIII]/H\beta$ and $[NeIII]/[OII]$ (e.g. Cresci et al. 2010). Using the spatially resolved data of SINFONI, Queyrel et al. (2012) determined metallicity gradients in 29 galaxies of the MASSIV sample at $z \sim 1.3$. They found seven unambiguous positive metallicity gradients, five of them being in interaction. Therefore, they interpreted their positive gradients as the signature of fresh gas being accreted in the centre do to tidal tails, which would dilute the inner metallicity. Positive gradients of the gaseous phase have not been observed yet in the local Universe. However, e.g. Rupke et al. (2010) have shown that strongly interacting galaxies have on average flatter gradients in their gaseous phase than isolated galaxies in the local Universe, which supports the interpretation provided by Queyrel et al. (2012). At higher redshift ($z \sim 3$), Cresci et al. (2010) also observed positive metallicity gradients in three rotating galaxies of the LSD/AMAZE sample, also from SINFONI data. According to them, the fact that these galaxies do not show evidence for interaction favours a scenario in which cold flows along cosmic filaments toward the centre are diluting the inner metallicity.

These different scenarios have to be confirmed both by more observations but also from numerical simulations including metallicity evolution for interacting galaxies and cosmological inflows.

5 Instrumental perspectives

Nowadays, almost each telescope has the possibility to make IFS observations. Tunable filter instruments have recently been installed on large telescopes such as Grantecan (OSIRIS) and SALT (RSS). They have a very large field of view (>5') and a tunable spectral resolution (from a few hundreds to a few thousands). New generations of IFS are also about to be installed on the largest telescopes. MUSE/VLT, will have both a large field of view (1') and spectral range, whereas KMOS/VLT will be able to deploy small integral field units (3") over a very large field of view (7'). Therefore, they will be adapted to different observing programs. Integral field instruments are not limited to optical and visible wavelengths. Indeed, radio telescope interferometers also enable to have both spatial and spectral information. New generation instruments such as ALMA and SKA will respectively enable to observe molecular and neutral gas for a very large number of galaxies, giving new insights in galaxy evolution.

References

Bacon, R., Copin, Y., Monnet, G., et al. 2001, MNRAS, 326, 23
Bournaud, F. & Elmegreen, B. G. 2009, ApJ, 694, L158
Cappellari, M., Emsellem, E., Krajnović, D., et al. 2011, MNRAS, 413, 813
Contini, T., Garilli, B., Le Fèvre, O., et al. 2012, A&A, 539, A91
Cresci, G., Mannucci, F., Maiolino, R., et al. 2010, Nature, 467, 811
de Zeeuw, P. T., Bureau, M., Emsellem, E., et al. 2002, MNRAS, 329, 513
Dekel, A., Birnboim, Y., Engel, G., et al. 2009, Nature, 457, 451
Dicaire, I., Carignan, C., Amram, P., et al. 2008, MNRAS, 385, 553
Dutton, A. A., van den Bosch, F. C., Faber, S. M., et al. 2011, MNRAS, 410, 1660
Emsellem, E., Cappellari, M., Krajnović, D., et al. 2011, MNRAS, 414, 888
Epinat, B., Amram, P., Balkowski, C., & Marcelin, M. 2010, MNRAS, 401, 2113
Epinat, B., Amram, P., & Marcelin, M. 2008, MNRAS, 390, 466
Epinat, B., Tasca, L., Amram, P., et al. 2012, A&A, 539, A92
Förster Schreiber, N. M., Genzel, R., Bouché, N., et al. 2009, ApJ, 706, 1364
Gnerucci, A., Marconi, A., Cresci, G., et al. 2010, ArXiv e-prints
Gonçalves, T. S., Basu-Zych, A., Overzier, R., et al. 2010, ApJ, 724, 1373
Green, A. W., Glazebrook, K., McGregor, P. J., et al. 2010, Nature, 467, 684
Krajnović, D., Cappellari, M., de Zeeuw, P. T., & Copin, Y. 2006, MNRAS, 366, 787
Law, D. R., Steidel, C. C., Erb, D. K., et al. 2009, ApJ, 697, 2057
Le Tiran, L., Lehnert, M. D., Di Matteo, P., Nesvadba, N. P. H., & van Driel, W. 2011, A&A, 530, L6
Lehnert, M. D., Nesvadba, N. P. H., Le Tiran, L., et al. 2009, ApJ, 699, 1660
López-Sanjuan, C., Balcells, M., Pérez-González, P. G., et al. 2009, A&A, 501, 505

Queyrel, J., Contini, T., Kissler-Patig, M., et al. 2012, A&A, 539, A93
Rupke, D. S. N., Kewley, L. J., & Chien, L.-H. 2010, ApJ, 723, 1255
Tresse, L., Ilbert, O., Zucca, E., et al. 2007, A&A, 472, 403
Wright, S. A., Larkin, J. E., Law, D. R., et al. 2009, ApJ, 699, 421
Yang, Y., Flores, H., Hammer, F., et al. 2008, A&A, 477, 789